



# Capacitive pressure sensor with monolithically integrated CMOS readout circuit for high temperature applications

Klaus Kasten<sup>a,\*</sup>, Norbert Kordas<sup>b</sup>, Holger Kappert<sup>b</sup>, Wilfried Mokwa<sup>a,b</sup>

<sup>a</sup>*Institute of Materials in Electrical Engineering I, RWTH Aachen, Sommerfeldstr. 24, D-52074 Aachen, Germany*

<sup>b</sup>*Fraunhofer Institute of Microelectronic Circuits and Systems, Duisburg, Germany*

Received 15 June 2001; received in revised form 30 October 2001; accepted 30 October 2001

## Abstract

An integrated capacitive surface micromachined pressure sensor for high temperature applications was developed and characterized to work at temperatures up to 250 °C. The sensor and the CMOS readout circuit are processed on separation by implantation of oxygen (SIMOX) substrates. The readout circuit is programmable and allows calibration of linearity, offset and output range. The performance of a 20 and 50 bar sensor is discussed. Even without active temperature compensation the offset temperature coefficient (TCO) referred to full scale output (FSO) is less than 0.03%/°C between 25 and 150 °C and less than 0.09%/°C between 150 and 250 °C. The compensated linearity error is less than 0.4% FSO. © 2002 Published by Elsevier Science B.V.

**Keywords:** High temperature application; Monolithic integration; Pressure sensor; Surface micromachining; SIMOX; SOI

## 1. Introduction

There is an increasing need for sensors and electronic devices working at temperatures beyond 125 °C. Typical applications are found in the automotive industry, in avionics and space exploration as well as in the oil drilling industry, industrial measurement and control systems. Several approaches have been made to solve the well known problem of the rising leakage current at high temperatures in conventional silicon devices using isolation by reverse biased p–n-junctions.

A promising approach for high temperature applications is the use of a wide bandgap semiconductor such as silicon carbide (SiC). The excellent electrical and mechanical properties at temperatures far beyond 350 °C make it a suitable material for electromechanical sensors in high temperature applications [1]. However, the rather expensive process technology is still a drawback for many commercial applications. Taking advantage of the highly developed and investigated silicon technology, another promising approach is the silicon on insulator (SOI) technology. Several designs

of piezoresistive pressure sensors have already been introduced on different SOI-substrates [2]. However, piezoresistive sensors have the disadvantage of an inherent temperature dependence of the piezoresistive coefficient, which has to be compensated. Using capacitive sensors this step can be avoided, because the pressure is converted to an electrical signal by a vacuum capacitor, which has no inherent temperature dependence. However, capacitive sensors need a readout circuit to convert the capacitance into a voltage. The monolithic integration of a readout circuit with the sensor offers the following advantages compared to a hybrid structure:

- short signal paths between sensor and readout circuit;
- small dimensions of the sensor system;
- omission of the connection technique between sensor and readout circuit, which results in:
  - smaller electrical and mechanical susceptibility to interference of the total system and;
  - reduction of the production costs with high numbers of items.

Within the area of capacitive high temperature pressure sensors with readout circuit the highest application temperature of 200 °C was achieved by a hybrid sensor system [3]. The CMOS-compatibility of the capacitive pressure sensor [4] allows us to integrate a high temperature readout circuit together with the sensing cells.

\* Corresponding author. Present address: Robert Bosch GmbH, AE/SPP2, Tuebingerstr. 123, D-72762 Reutlingen, Germany.  
Tel.: +49-7121-35-6626; fax: +49-7121-35-4934.  
E-mail address: klaus.kasten2@de.bosch.com (K. Kasten).

## 68 2. Sensor principle and circuit design

69 The capacitive sensor consists of an array of circular  
70 pressure sensitive membranes, which serve as the top electro-  
71 des. The membranes are switched in parallel to increase  
72 the value of the capacitance. The pressure range of the sensor  
73 is determined by the diameter of the membranes. There are  
74 two arrays of membranes on each chip, which only differ in  
75 the membrane thickness. This results in a pressure sensitive  
76 sensor array and a pressure insensitive reference array.  
77 Hence, the sensor signal is gained by the ratio of reference  
78 to sensor capacitance, which is almost free from thermal  
79 dependencies of the parasitic capacitances.

80 Fig. 1 shows a cross section of a sensor and a reference  
81 element. The bottom electrode is built from a 120 nm silicon  
82 layer and electrically isolated from the substrate by the  
83 underlying buried silicon oxide layer. Lateral isolation is  
84 achieved by a localized oxidation of silicon (LOCOS)  
85 process. These dielectrics replace the p–n-junctions used  
86 by Dudaicevs et al. [5] and guarantee low leakage currents at  
87 temperatures beyond 125 °C.

88 The cavity with a height of 900 nm under the membrane  
89 is defined by a sacrificial oxide, which is removed via etch  
90 channels by means of hydrofluoric acid. Afterwards it is  
91 sealed in an LPCVD deposition process. Due to the LPCVD  
92 process the remaining pressure inside the sealed cavity is  
93 around  $10^{-4}$  bar. Compared to the pressure ranges of the  
94 discussed sensors (20 and 50 bar) this is negligible and we  
95 can assume vacuum inside the cavity. Thus, the membranes  
96 are sensitive for absolute pressure. The readout circuit has  
97 been fabricated in a 1.6  $\mu\text{m}$  separation by implantation of

98 oxygen (SIMOX)-CMOS process technology with 40 nm  
99 gate oxide, suitable for high temperature applications [6].

100 In Fig. 2 the comparison of a Bulk CMOS cell with a SOI-  
101 CMOS cell is shown. The isolation of the individual trans-  
102 istors of the Bulk CMOS cell is achieved by means of p–n-  
103 junctions to the p-substrate (NMOS transistor) or to an n-tub  
104 (PMOS transistor). These p–n-junctions serve as a sufficient  
105 electrical isolation up to temperatures of approximately  
106 150 °C. Beyond this temperature the leakage currents to  
107 the substrate caused by the intrinsic conductivity of silicon  
108 are rising strongly. Exceeding a certain limit, these leakage  
109 currents cause the failure of the whole circuit. The replace-  
110 ment of the p–n-junctions by dielectric isolation reduces the  
111 leakage currents around 3 to 4 orders of magnitude [7]. In  
112 this way the temperature range of the CMOS circuits can be  
113 extended well over 150 °C. The boundary of operability is  
114 then defined by leakage currents within a transistor. Depend-  
115 ing upon the type of circuit this boundary is between 250 and  
116 350 °C for analog SOI circuits. While operation amplifier  
117 circuits can be operated up to 350 °C, the accuracy of  
118 switched capacitor (SC) circuits drops rapidly beyond  
119 250 °C. The reason is the strong increase of the drain leakage  
120 current in the transmission gates, which amounts to several  
121 nanoampere at 300 °C [8].

122 The design of the readout circuit is based on SC techni-  
123 que. This technique is used for the capacitance to voltage ( $C/V$ )  
124 converter as well as for the linearization and signal  
125 conditioning. To get a time continuous output signal the  
126 output stage is realized as a sample and hold amplifier. Fig. 3  
127 shows a block diagram of the complete sensor system. The  
128 first stage represents the  $C/V$  converter (Cr/Cs) and performs

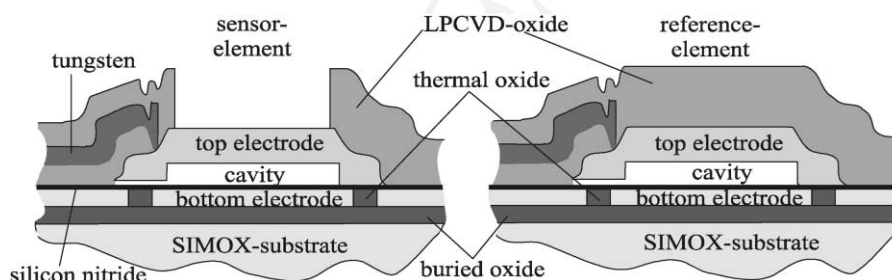


Fig. 1. Schematic cross-section of a sensor and reference element.

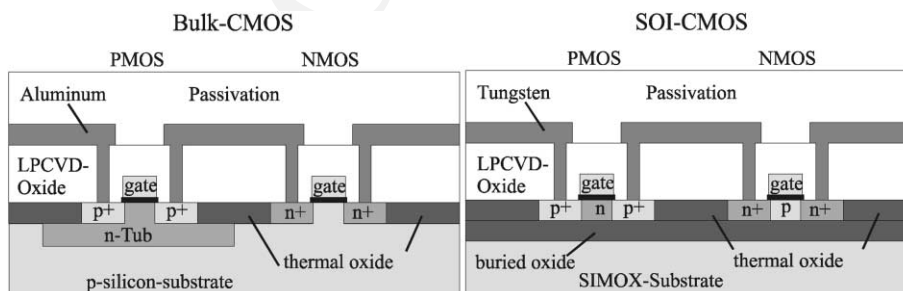


Fig. 2. Schematic cross-section of a bulk CMOS cell and an SOI-CMOS cell.

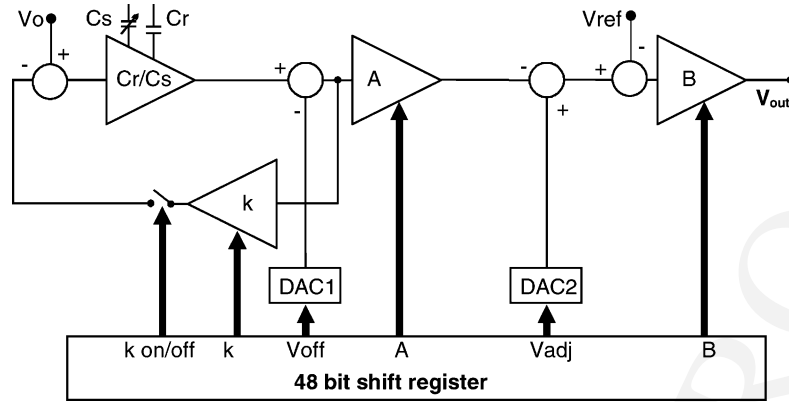


Fig. 3. Block diagram of the sensor system.

129 the linearization via a feedback path. The feedback path is  
 130 implemented with an additional operation amplifier ( $k$ ). This  
 131 stage creates a pressure proportional output signal. The  
 132 second and third stage ( $A$ ,  $B$ ) are used for further amplifica-  
 133 tion and adjustment of the output range.

134 All amplification factors ( $A$ ,  $B$ ,  $k$ ) and offset voltages ( $V_{off}$ ,  
 135  $V_{adj}$ ) are programmable by a 48 bit shift register. This allows  
 136 the combination of one readout circuit design with various  
 137 sensor elements to attain different pressure ranges. The  
 138 output voltage of the first DAC ( $V_{off}$ ) is used to compensate  
 139 the zero pressure output signal, which varies due to mis-  
 140 match between sensor and reference elements. The second  
 141 DAC ( $V_{adj}$ ) is added to adjust the range of the output signal.  
 142 Considering the transfer function of the  $C/V$  converter

$$V_{C/V} = V_{DD} - (V_{DD} - V_0) \frac{C_r}{C_s} \quad (1)$$

144 the overall transfer function results to:

$$V_{out} = \left\{ \frac{V_{DD} - (V_{DD} - V_0)C_r/C_s - V_{off}}{1 - k(C_r/C_s)} A + V_{adj} - V_{ref} \right\} B \quad (2)$$

147

Fig. 4 shows a chip photo of the integrated sensor system. On the upper left side there is the array of circular pressure sensitive membranes, while on the right side the same array with thicker membranes can be seen.

### 3. Experimental results

#### 3.1. Linearization

For the linearization of the pressure sensor, two steps have been taken. Firstly, as the capacitance value is inversely proportional to the distance between the membrane and the bottom electrode, the quotient of the reference capacitance to the sensor capacitance is used. Secondly, to compensate the remaining non-linearity, an analog feedback has been added to the converter stage. Fig. 5 compares the output signals with and without feedback stage of a 20 bar sensor. The curve without feedback stage (non-linearized) has an independent linearity error of 9.42% referred to full scale output (FSO). The linearization by the feedback stage reduces the linearity error to less than 0.4% FSO.

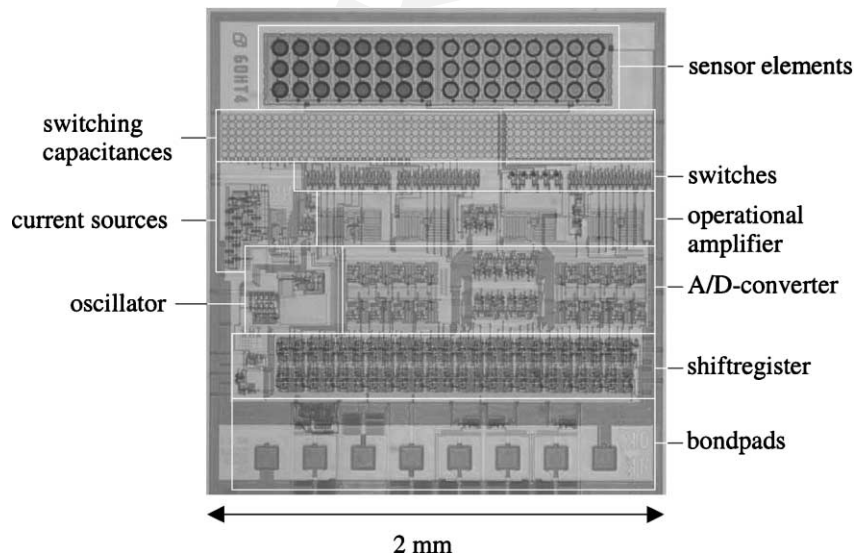


Fig. 4. Chip photo of the integrated sensor. The individual function groups are emphasized and designated.

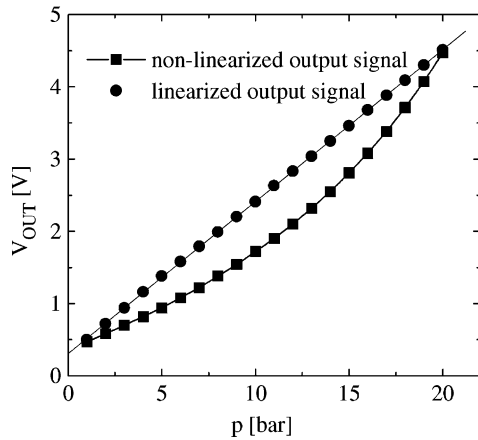


Fig. 5. Linearization of the output signal by means of the feedback stage.

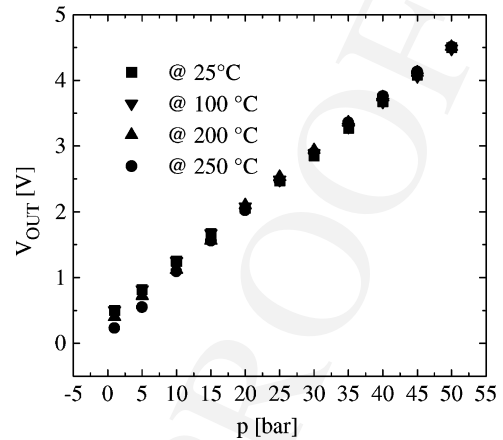


Fig. 7. Linearized output signals at different temperatures.

166 In order to minimize the linearization error, a highly  
 167 accurate adjustment of the value  $k$  is required. In the pre-  
 168 sented design  $k$  is programmable with a resolution of 6 bit by  
 169 the shift register. Fig. 6 shows the influence of a gradual  
 170 modification of  $k$  on the linearity error in the proximity of the  
 171 minimum. In the area  $\pm 1$  bit apart from the minimum at 31  
 172 the linearization error remains smaller than 0.5% FSO.  
 173 Therefore the modification of  $k$  with the given digital  
 174 resolution permits a good detection of the minimum.

175 *3.2. Temperature dependencies*

176 In the following the thermal behaviour of a 50 bar sensor  
 177 in the temperature range between 25 and 250 °C will be  
 178 discussed. Fig. 7 shows the linearized output signals of a  
 179 50 bar sensor at different temperatures. The output signal is  
 180 adjusted to a range from 0.5 to 4.5 V. The measuring points  
 181 at different temperatures lie on top of each other well. Only  
 182 at low pressures and high temperatures there is a recogniz-  
 183 able deviation.

184 To have a closer look at the deviation Fig. 8 plots the  
 185 temperature dependencies of the output signal at different

pressures. The output signals at higher pressures show a very  
 low temperature dependence over the whole temperature  
 range. At a pressure of 1 bar the signal drops at temperatures  
 beyond 150 °C. To quantify this behaviour the offset tem-  
 perature coefficient (TCO) was determined with the follow-  
 ing formula:

$$TCO = \frac{\partial V_{out}}{\partial T} \frac{1}{V_{FSO}} \quad (3)$$

The TCO equals to the temperature derivative of the output  
 signal referred to the full scale output ( $V_{FSO}$ ). The full scale  
 output is the difference between the minimum and max-  
 imum output signal, which is in this case:  $V_{FSO} =$   
 $4.5 - 0.5 = 4$  V.

Fig. 9 plots the temperature dependencies of the TCO at  
 different pressures. At 50 bar the TCO is less than 0.01%  
 FSO/°C over the whole temperature range. At a pressure of  
 25 bar the TCO is still less than 0.03% FSO/°C over the  
 whole temperature range. The strongest temperature depen-  
 dence was observed at the lowest pressure, where sensor and  
 reference capacitance have nearly the same value. Up to a  
 temperature to 150 °C the TCO is still less than 0.03% FSO/  
 206

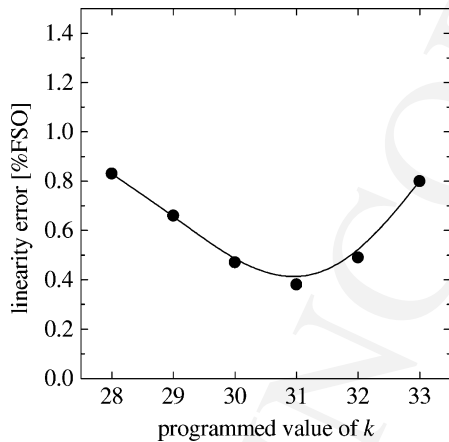


Fig. 6. Linearity error of a 20 bar sensor as a function of the programmed value of the feedback factor  $k$ .

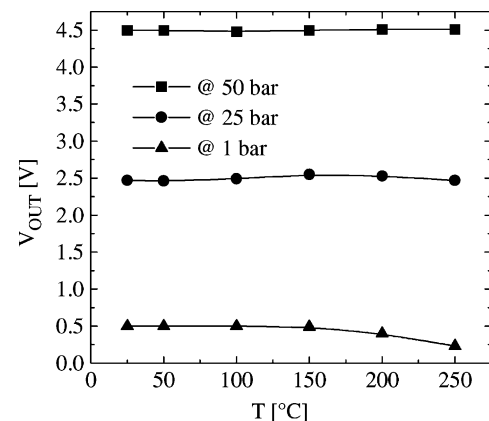


Fig. 8. Temperature dependencies of the output signal at different pressures.

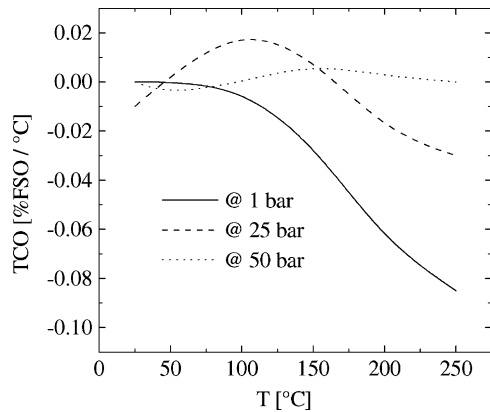


Fig. 9. Temperature dependencies of the offset temperature coefficient at different pressures.

207 °C, but raises to less than 0.09% FSO/°C at 250 °C. As  
 208 shown in [4], the offset TCO of the actual sensor elements is  
 209 less than 0.015% FSO/°C in the temperature range between  
 210 25 and 250 °C. This seems to suggest that the temperature  
 211 dependence at lower pressures and higher temperatures may  
 212 be caused by the readout circuit.

#### 213 4. Conclusions and outlook

214 It has been shown that a surface micromachined pressure  
 215 sensor with a monolithically integrated CMOS readout  
 216 circuit is capable of measuring at temperatures up to  
 217 250 °C. The linearity error is less than 0.4% FSO at room  
 218 temperature. Even without active temperature compensation  
 219 the offset TCO is less than 0.03% FSO/°C between 25 and  
 220 150 °C and less than 0.09% FSO/°C between 150 and  
 221 250 °C. Future improvements will concentrate on the  
 222 remaining temperature dependence at low pressures. The  
 223 next version will also contain a high temperature EEPROM  
 224 [6] for the permanent storage of calibration data.

#### References

- 226 [1] Pasqualina M. Sarro, Silicon carbide as a new MEMS technology,  
 227 in: Proceedings of the Transducers'99, Sendai, Japan, 1999, pp. 186–  
 228 189.  
 229 [2] B. Diem, P. Rey, S. Renard, S. Violet Bosson, H. Bono, F. Michel,  
 230 M.T. Delaye, G. Delapierre, SOI, SIMOX, from bulk to surface  
 231 micro-machining, a new age for silicon sensors and actuators, Sens.  
 232 Actuators A46/A47 (1995) 8–16.  
 233 [3] S.T. Moe, K. Schjolberg-Henriksen, D.T. Wang, E. Lund, J.  
 234 Nysaether, L. Furuberg, M. Visser, T. Fallet, R.W. Bernstein,  
 286

- Capacitive differential pressure sensor for harsh environments, Sens.  
 Actuators A83 (1–3) (2000) 30–33. 235  
 [4] K. Kasten, J. Amelung, W. Mokwa, CMOS-compatible capacitive  
 high temperature pressure sensors, Sens. Actuators A85 (2000) 147–  
 152. 236  
 [5] H. Dudaicevs, M. Kandler, Y. Manoli, W. Mokwa, E. Spiegel,  
 Surface micromachined pressure sensors with integrated CMOS  
 read-out electronics (Transducers'93, Yokohama 1993), Sens.  
 Actuators A 43 (1994) 157–163. 237  
 [6] D. Gogl, H.-L. Fiedler, M. Spitz, B. Parmentier, A 1-Kbit EEPROM  
 in SIMOX technology for high-temperature applications up to 250  
 °C, IEEE J. Solid State Circuits, 35 (10) 1387–1395. 238  
 [7] D. Gogl, G. Burbach, H.-L. Fiedler, M. Verbeck, C. Zimmermann, A  
 single-poly EEPROM cell in SIMOX technology for high temperature  
 applications up to 250 °C, IEEE Electron Device Lett. 18 (1997)  
 541–543. 239  
 [8] M. Verbeck, Hochttemperaturtaugliche, Analoge Schaltungskompo-  
 nenten in SIMOX-Technologie, Ph.D. Thesis, University of Duis-  
 burg, Duisburg, 1997. 240  
 241  
 242  
 243  
 244  
 245  
 246  
 247  
 248  
 249  
 250  
 251  
 252  
 253

#### Biographies

*Klaus Kasten* was born in Gladbeck, Germany, in 1968. He obtained his  
 diploma in electrical engineering from the Technical University (RWTH)  
 of Aachen, Germany, in 1996. He joined the Institute of Materials in  
 Electrical Engineering in 1996, working on the design, packaging and  
 testing of high temperature pressure sensors. Since September 2001 he is  
 with the Robert Bosch GmbH, where he is working on the development of  
 new sensor products for automotive applications. 255  
 256  
 257  
 258  
 259  
 260  
 261

*Norbert Kordas* was born in Herten, Germany and received the Diploma in  
 electrical engineering from the University of Dortmund in 1988 and the  
 Doctorate degree in engineering from the University of Duisburg in 1994.  
 He is with the Fraunhofer Institute of Microelectronic Circuits and  
 Systems in Duisburg, where his special interests are mixed mode CMOS  
 circuits and sensor readout electronics. 262  
 263  
 264  
 265  
 266  
 267

*Holger Kappert* was born in 1968. He has received the Diploma in  
 electrical engineering from the University of Bochum in 1993. Since  
 then he is with the Fraunhofer Institute of Microelectronic Circuits  
 and Systems, where he is working on embedded mixed signal systems.  
 His special research interest is the design for testability of those  
 systems. 268  
 269  
 270  
 271  
 272  
 273

*Wilfried Mokwa* was born in 1951. He obtained the Diploma in physics  
 from the Technical University (RWTH) of Aachen, Germany, in 1977 and  
 the Dr. rer. nat. degree in 1981 at the same place. From 1981 he worked at  
 the Department of Experimental Condensed Matter Physics at the RWTH  
 Aachen on catalytic reactions on gas sensor surfaces and joined the  
 Fraunhofer Institute of Microelectronic Circuits and Systems (IMS) in  
 Duisburg in 1985. There he managed a group working on integrated silicon  
 sensor technology. In 1996 he became a full professor in electrical  
 engineering at the RWTH Aachen where he is head of chair 1 of the  
 Institute of Materials for Electrical Engineering with special interests in  
 the field of integration of microsystems. At the same time he is still  
 managing the microsystems activities of the IMS. 274  
 275  
 276  
 277  
 278  
 279  
 280  
 281  
 282  
 283  
 284  
 285